ISSN 1027-4510, *Journal of Surface Investigation: X-ray, Synchrotron and Neutron Techniques, 2023, Vol. 17, No. 6, pp. 1248–1252. © Pleiades Publishing, Ltd., 2023.*
Russian Text © The Author(s), 2023, published in Poverkhnost', 2023, No. 11, pp. 78–83.

Superconducting Solenoid (7 T) Indirectly Cooled by Cryocoolers for THz Radiation

A. V. Bragin[a, *], **A. A. Volkov**[a, b], **V. V. Kubarev**[a], **N. A. Mezentsev**[a, b],
O. A. Tarasenko[a], **S. V. Khrushchev**[a, b], **V. M. Tsukanov**[a, b], **and V. A. Shkaruba**[a, b]

[a] *Budker Institute of Nuclear Physics, Siberian Branch, Russian Academy of Sciences, Novosibirsk, 630090 Russia*
[b] *Center for Collective Use "Siberian Circular Photon Source" (SKIF), Boreskov Institute of Catalysis, Siberian Branch, Novosibirsk, 630559 Russia*
**e-mail: bragin@inp.nsk.su*

Received December 1, 2022; revised February 10, 2023; accepted February 10, 2023

Abstract—The results of testing and performance characteristics of an indirectly cryocooled superconducting solenoid to be used at the tehrahertz (THz) spectroscopy experimental station of the free-electron laser at the Institute of Nuclear Physics are presented. The superconducting solenoid with a winding diameter of 102 mm and a length of 0.5 m is designed for a magnetic field of 6.5 T. A warm diameter of 80 mm is available for THz spectroscopy experiments. A superconducting wire Cu/NbTi = 1.4 is used. The design implements passive protection methods due to sectioning and secondary connected circuits in case of a sudden quench. The required field uniformity of 0.5% is ensured by using an iron yoke and additional side windings. The cryogenics of the solenoid is based on two Sumitomo HI cryocoolers. The solenoid and iron yoke are cooled by the second stage of the cryocooler via copper plates. The manufacturing technology of the solenoid is described in detail. The solenoid is tested in a liquid-helium bath and in its own cryostat. Its characteristics meet the requirements of the experimental station. The obtained field of 7.3 T is greater than the designed one due to overcooling up to 3.6 K. The magnetic field is measured both in a bath cryostat and in the designed cryostat; the results corresponded to the design calculations. The solenoid cooling time is 13 days. The quench happened only twice, at 5.6 and 7.3 T.

Keywords: superconducting solenoid, terahertz radiation, indirectly cooled superconducting magnet, passively protected superconducting magnet, high-magnetic-field magnet

DOI: 10.1134/S1027451023060071

INTRODUCTION

The superconducting solenoid will be used at the free-electron laser experimental station operating at the Institute of Nuclear Physics [1–3]. The features and relevance of experiments on terahertz spectroscopy, as well as the need to use a solenoid that generates a strong magnetic field with increased homogeneity, were discussed in [4–7].

The superconducting solenoid was designed in accordance with the requirements for experiments on terahertz spectroscopy [8]. Its main parameters are as follows. It should provide a magnetic field of more than 6 T in a heated channel 80 mm in diameter over a length of 0.2 m with a uniformity of less than 0.5% in this space. A cryogenic system based on cryocoolers is necessary for ease of operation, so the magnet design is attached directly to the cryocooler using copper plates. For the operation of such a cryogenic system, only electricity and pure industrial water are needed.

MAGNET DESIGN

The principal arrangement of a magnet consisting of a solenoid and an iron yoke is described at the conceptual level in [8]. The specific type of magnet and its layout during assembly are shown in Fig. 1. The solenoid is assembled in its own cryostat, which includes a vacuum chamber, radiation shields, two cryocoolers, current leads, and an iron yoke. The current leads consist of resistive brass rods of optimized length and cross section and superconducting inserts made of HTSC tape. The inserts were made by SuperOx.

Two cryocoolers SRDK-408S2 and SRDK-408D2 manufactured by Sumitomo HI were used to cool the magnet. The maximum cooling power of the cryocoolers was 1 W at 4.2 K, 14 W at 20 K, and 85 W at 50 K.

The design contains two radiation screens made of copper sheets 3 mm thick. Their calculated temperatures were ~60 and 20 K, respectively. Between the inner diameter of the solenoid and the vacuum chamber there was only a 20-K radiation screen. The radiation screens were thermally connected to the cryo-

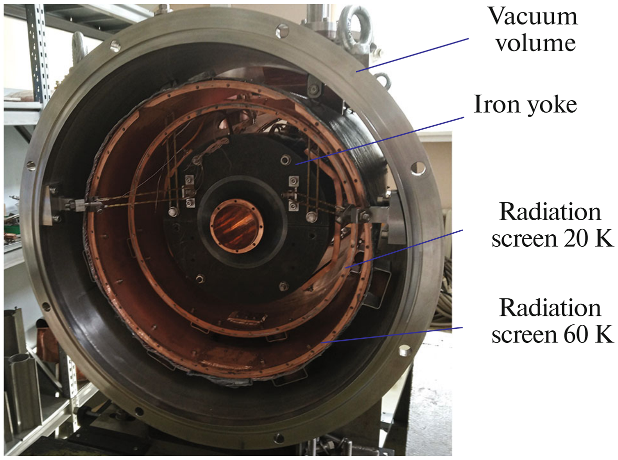

Fig. 1. Solenoid during assembly and its components.

cooler stages by flexible copper bridges. The 60-K radiation-screen assembly is supported by plastic balls and abuts the vacuum volume. In the same way, the 20-K screen assembly rests against the 60-K radiation screen. The outer surfaces of the 60-K radiation shield were covered with 20 layers of multilayer superinsulation. The material of the shields is 99.9% copper.

The material of the iron yoke is low-carbon steel of type 08kp. The solenoid is bolted to the iron yoke from only one end to prevent thermal stresses due to the difference in the coefficients of thermal expansion of the dissimilar materials. The magnet is suspended from the vacuum vessel using vertical and horizontal threads made of Kevlar-type material (Fig. 1).

On the whole, the approach to designing a cryostat is the same as for superconducting wigglers implemented by the authors over many years [9]. Experience in designing indirectly cooled superconducting magnets was obtained in [10] and on a test bench.

Fig. 2. Solenoid after impregnation with the epoxy compound.

STRUCTURE OF THE SUPERCONDUCTING WINDING

At the design stage, the dimensions of the superconducting winding and the iron yoke were optimized using the ANSYS program [11]. The main parameters of the solenoid are listed in Table 1.

The winding was fabricated using a composite wire based on a NbTi superconductor in a copper matrix. The bare-wire diameter was 0.87 mm and the Cu/NbTi ratio was 1.43. Its insulated diameter was 0.92–0.93 mm. The critical current of the wire at 5 T and 4.2 K is about 360 A. The number of strands in the wire is NbTi 8920 with a diameter of ~6 μm. The total length of the wire, about 4.2 km, was twice as long as the available manufactured wire in reels, so the winding was spliced only once and thus divided into two sections. This joining of the sections was carried out by soldering with PbSn-61 solder over a length of ~40 cm along the outer surface of the winding (Fig. 2).

The wire is wound on a copper cylinder made of commercial copper M1. Before winding the wire, the surface of the cylinder was covered with insulation with a total thickness of ~0.5 mm with G-10 material. The flanges of the copper cylinder are grooved for laying wire inputs and outputs and for epoxy impregnation. After the winding of 20 layers was completed, a

Table 1. Main design parameters of the solenoid

Parameter	Meaning
Winding inner diameter, mm	101
Winding length, mm	500
Heated diameter for placing samples, mm	80
Number of turns	11560
Number of turns (+ at the ends of the solenoid)	20 + 2
Peak field on the winding	6.62
Field at the center of the solenoid	6.5
Winding current, A	236
Ratio of operating current to critical current at 4.2 K (I_{oper}/I_{cr}), %	83
Inductance, H	3.31
Stored energy, kJ	92

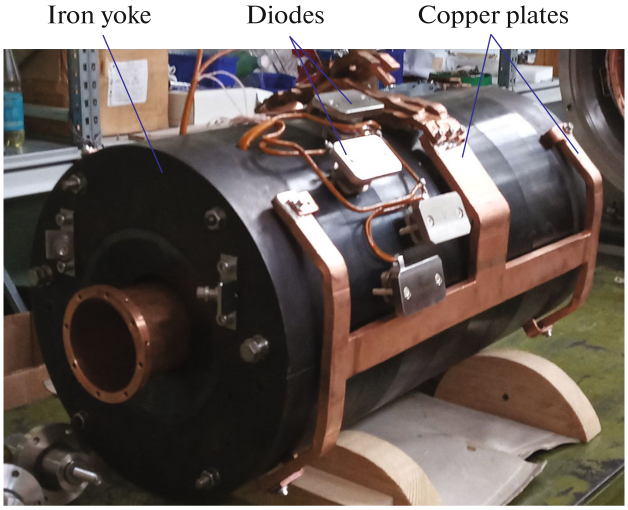

Fig. 3. Assembly of the solenoid before installation in the proprietary cryostat.

STEF-1 sheet 0.5 mm thick was wrapped four times around the outer surface of the solenoid, leaving a free space 80 mm long for additional side turns. These additional turns were wound from a second bobbin, i.e., without additional splicing. For smooth winding, helical grooves were cut in the outer sheets of G-10 (Fig. 2). Copper foil 1 mm thick was placed under these STEF-1 sheets to fix the temperature sensor.

After completion of the process of winding and soldering of the sections, the solenoid was impregnated with an epoxy compound consisting of aluminum-oxide powder with a grain size of ~5 μm and epoxy resin of the ED-16 type. For this purpose, the solenoid was placed in a rubber bag, filled with the compound, and kept at a temperature of 90°C and a pressure of ~18 bar for several hours. This technology has also been used in other works and has shown its effectiveness [12].

The solenoid was assembled with an iron yoke as shown in Fig. 3. Each flange of the copper cylinder of the solenoid has four copper plates connected to the second stage of the cryocooler by means of flexible copper plates.

SOLENOID PROTECTION

In the event of sudden quench to the normal state, high temperatures and electrical stress can occur in the solenoid, which can lead to structural failure. To minimize and eliminate these effects, the protection of superconducting devices is used, which is aimed at ensuring a uniform temperature distribution and the output of stored energy to external elements.

Protection of this solenoid is based on passive methods, namely, winding sectioning was used, and secondary circuits were also involved in the design. The solenoid was sectioned using diodes (Figs. 3, 4). Diode shunts were installed on each section of the solenoid. The section contained a superconducting winding wire ~2.2 km long. Although there are only two sections, such a scheme will contribute to a more uniform distribution of the stored energy during the quench of the solenoid to the normal state.

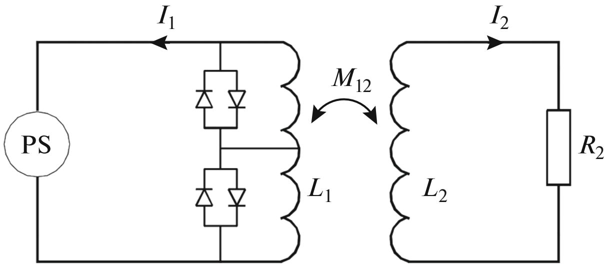

Fig. 4. Electrical circuit of the solenoid protection for the case of quench back. Parameters L_2 and R_2 characterize the secondary circuit.

Secondary circuits were used according to the theory described in [13, 14]. In this design of the solenoid, a copper cylinder, a 20-K radiation screen, and an iron yoke were considered as secondary circuits. Secondary circuits make it possible to remove part of the stored energy from the power supply–solenoid circuit, and also significantly reduce the electrical voltage in the circuit.

The ANSYS program was used to calculate the transverse velocity of the normal zone along the superconducting wire, which was ~1.5 m/s. The copper cylinder will accelerate the interturn velocity of normal-zone propagation due to the direct heating of nearby turns of the solenoid (quench-back effect). In calculations using analytical formulas, the effect of secondary circuits was estimated [14]. As a result of the transient analysis, a hot-spot temperature of less than 120 K was obtained, which indicates good protection of the solenoid.

TESTS

The magnet was tested in a liquid-helium bath at 4.2 K and in its own cryostat. In a liquid-helium bath, the solenoid was tested up to 6.5 T at a low current-input rate of ~0.05–0.1 A/s. There was only one training quench to the normal state during the first powering up of the solenoid at a current of 205 A, corresponding to ~5.6 T. The field map was measured at several current values using five Hall sensors installed along the solenoid radius and scanning along the solenoid axis. The measurement results are shown in Fig. 5; they meet the requirements for the magnet.

The proprietary cryostat was also equipped with a power supply, temperature sensors, and a control system that allowed all measurements to be made and the quench to normal to be detected. Temperature sensors for the range of 3–300 K were installed on the outer layer of the winding, on the copper cylinder, on the iron yoke, and on the second stage of the cryocooler. Sensors for the range of 20–300 K are installed on the first stages of the cryocoolers, current leads, and radiation shields.

After the assembly of the solenoid was completed, the cryostat was cooled by cryocoolers to a temperature below 4.2 K over 13 days. A heavy iron yoke determined the cooling time. The solenoid temperature before current injection was ~3.6 K. Current input was carried out up to 7.3 T without a quench to the normal state. The magnetic field was measured at several currents, and some of the results are shown in Fig. 5, which meets the requirements for the magnet. The solenoid was tested for several days to measure the magnetic field and align the solenoid with respect to the axis of the cryostat.

In order to be sure that the solenoid would work at the terahertz spectroscopy station, it was decided to induce a quench to the normal state by injecting a current at a high rate of 7 T. Under these conditions, the solenoid went to the normal state at 7.3 T, which corresponds to a current of 271 A and a ratio of the operating current to the critical one of $I_{\text{oper}}/I_{\text{cr}}$ at 4.2 K, ~95%, while the solenoid temperature was below 4.0 K. The temperature behavior of the solenoid elements during the quench is shown in Fig. 6. After that, the solenoid was powered up to 7 T to demonstrate its performance.

RESULTS AND DISCUSSION

The solenoid reached its design parameters after one training quench to the normal state. Several design and manufacturing conditions led to these results. The winding, consisting of homogeneous materials, mainly copper, and the powdered epoxy compound used prevent large shrinkage stresses at the interface between different materials. The iron yoke significantly reduces axial forces, which can lead to coil delamination from the copper-frame flanges. In such a situation, the superconducting winding was mainly under the action of circumferential stresses, which are estimated at ~50 MPa, which is lower than the strength of the epoxy compound of ~100 MPa at low temperatures. It was decided to set the working magnetic field of the solenoid at a level of 7 T. The general view of the cryostat during testing is shown in Fig. 7.

The temperatures of the radiation shields were ~40 and 10 K due to the conservative approach in designing the cryostat. The analysis of the transition to the normal state was performed similarly to the previous experience of the authors [15]. It showed that, upon a quench with a field of 7.3 T, about 15% of the stored energy is dissipated in the 20-K screen and the iron yoke. A rapid increase in the temperature of the copper cylinder, the 20-K radiation screen, and the iron yoke indicates the appearance of eddy currents in

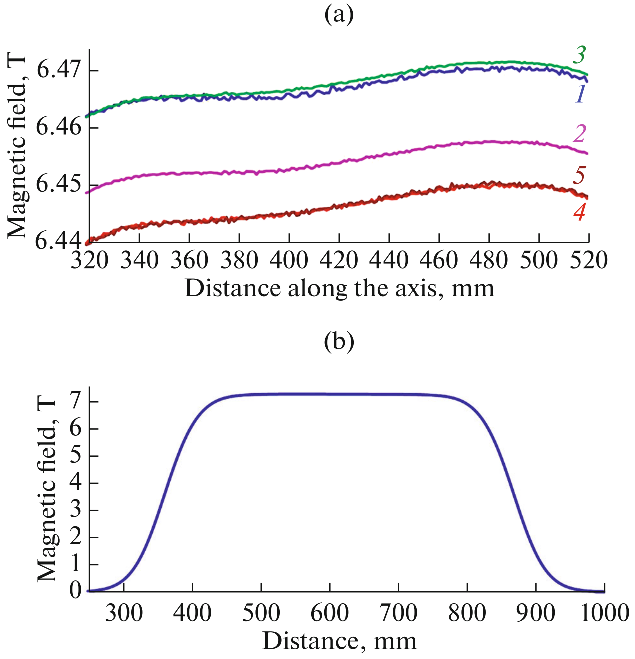

Fig. 5. Results of measurements of the magnetic field by five Hall sensors (*1–5*) in the solenoid during immersion tests at 240 A (a) and in the proprietary cryostat at 270 A (b).

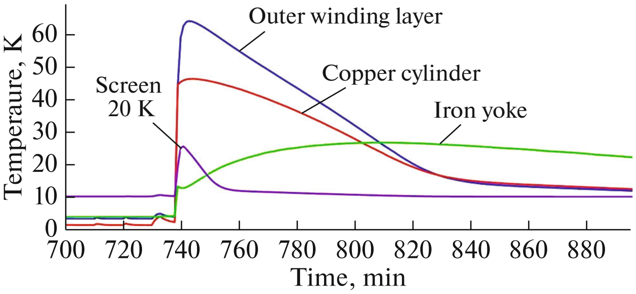

Fig. 6. Change in the temperature in the elements of the magnet after the quench to the normal state.

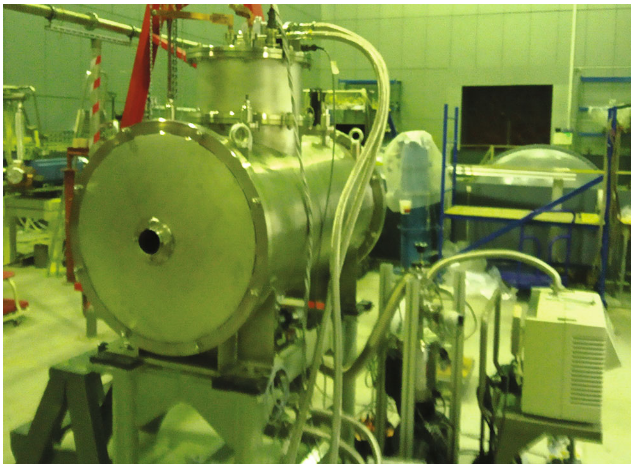

Fig. 7. Type of cryostat during testing.

these elements, which means that part of the stored energy was released to them. The amount of released energy can be estimated from the difference between the enthalpy values in these elements, ranging from 4 K to a temperature that sharply increased in less than 1 s (Fig. 6).

CONCLUSIONS

The solenoid with indirect cooling due to cryocoolers demonstrated its performance at 7 T and demonstrated the required uniformity of the magnetic field in the working area. The solenoid cooling time is 13 days. The quench-back protection was tested and analyzed only once during the triggered quench at 7.3 T. The solenoid is ready for use.

ACKNOWLEDGMENTS

We express our sincere gratitude to I. Gurgutsa, and V. Kazakov for assembling the cryostat and improving its design, G. Verkhovod and Yu. Toykichev for assembling the solenoid from the protection system and A. Pozdeev for manufacturing the solenoid.

FUNDING

The work was carried out under agreement no. 075-15-2021-1359 with the Ministry of Science and Higher Education of the Russian Federation and partly with the financial support of the Ministry of Science and Higher Education of the Russian Federation within the framework of the state task for the Institute of Solid State Chemistry and Mechanochemistry of the Siberian Branch of the Russian Academy of Sciences (project no. FWUS-2021-0004).

CONFLICT OF INTEREST

The authors state that they have no conflicts of interest.

REFERENCES

1. V. Kubarev, E. Chesnokov, and P. Koshlyakov, in *Proc. 37th Int. Conf. on Infrared, Millimeter and Terahertz Waves 2012* (Wollongong, 2012), p. Thu-C-2-4.
2. V. V. Kubarev, E. N. Chesnokov, and P. V. Koshlyakov, in *Proc. 38th Int. Conf. on Infrared, Millimeter and Terahertz Waves 2013* (Mainz on the Rhine, 2013), p. Tu5-5.
3. E. N. Chesnokov, V. V. Kubarev, and P. V. Koshlyakov, Appl. Phys. Lett. **105**, 261107 (2014).
4. E. N. Chesnokov, V. V. Kubarev, P. V. Koshlyakov, and G. N. Kulipanov, Appl. Phys. Lett. **101**, 131109 (2012).
5. E. N. Chesnokov, V. V. Kubarev, P. V. Koshlyakov, and G. N. Kulipanov, Laser Phys. Lett. **10**, 055701 (2013).
6. E. N. Chesnokov, V. V. Kubarev, and P. V. Koshlyakov, Laser Phys. Lett. **18**, 085205 (2021).
7. E. N. Chesnokov, V. V. Kubarev, L. N. Krasnoperov, and P. V. Koshlyakov, Phys. Chem. Chem. Phys. **22**, 20248 (2020).
8. A. V. Bragin, S. V. Khrushchev, V. V. Kubarev, N. A. Mezencev, V. M. Tsukanov, G. I. Sozinov, and V. A. Shkaruba, Phys. Procedia **84**, 82 (2016).
9. S. Khrushchev, N. Mezentsev, V. Lev, V. Shkaruba, V. Syrovatin, and V. Tsukanov, in *Proc. 5th Int. Particle Accelerator Conference* (Dresden, 2014), p. 4103. https://doi.org/10.18429/JACoW-IPAC2014-WEPRI091
10. A. V. Bragin, A. Bernhard, S. Casalbuoni, L. G. Fajardo, P. Ferracin, A. Grau, Ye. A. Gusev, S. Hillenbrand, S. V. Khrushchev, I. V. Poletaev, V. A. Shkaruba, D. Schoerling, V. M. Syrovatin, O. A. Tarasenko, V. M. Tsukanov, A. A. Volkov, K. V. Zolotarev, and N. A. Mezentsev, IEEE Trans. App. Supercond. **26**, 4102504 (2016).
11. http://www.ansys.com.
12. D. Schoerling, F. Antoniou, A. Bernhard, A. Bragin, M. Karppinen, R. Maccaferri, N. Mezentsev, Y. Papaphilippou, P. Peiffer, R. Rossmanith, G. Rumolo, S. Russenschuck, P. Vobly, and K. Zolotarev, Phys. Rev. Accel. Beams **15**, 042401 (2012).
13. M. A. Green, Cryogenics **24**, 3 (1984).
14. M. A. Green, Cryogenics **24**, 659 (1984).
15. A. V. Bragin, L. M. Barkov, N. S. Bashtovoj, A. A. Grebenuk, S. V. Karpov, V. S. Okhapkin, S. G. Pivovarov, Yu. S. Popov, A. A. Ruban, and B. I. Khazin, IEEE Trans. Appl. Supercond. **20**, 2336 (2010).